

# Structure–Enantioselectivity Relationship (SER) Study of Cinchona Alkaloid Chlorocyclization Catalysts

Sarah E. Luderer, Behrad Masoudi, Aritra Sarkar, Calvin Grant, Arvind Jaganathan, James E. Jackson,\* and Babak Borhan\*



Cite This: <https://doi.org/10.1021/acs.joc.3c00084>



Read Online

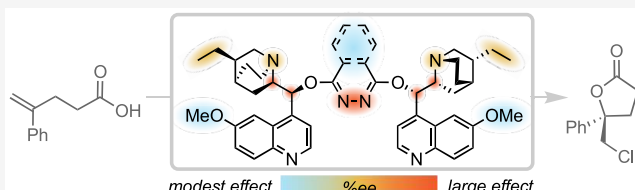
ACCESS |

Metrics & More

Article Recommendations

Supporting Information

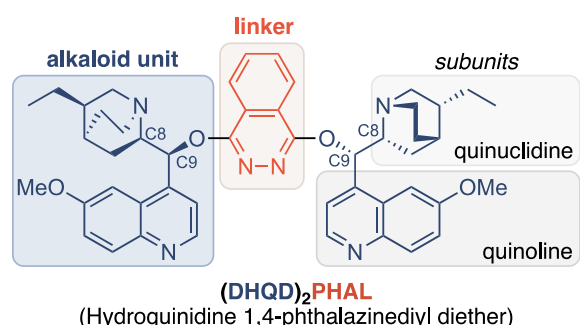
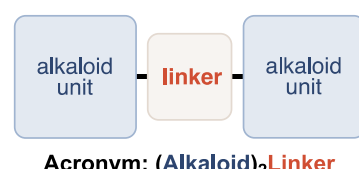
**ABSTRACT:** Various structural elements of the Cinchona alkaloid dimers are interrogated to establish a structure–enantioselectivity relationship (SER) in three different halocyclization reactions. SER for chlorocyclizations of a 1,1-disubstituted alkenoic acid, a 1,1-disubstituted alkeneamide, and a *trans*-1,2-disubstituted alkeneamide showed variable sensitivities to linker rigidity and polarity, aspects of the alkaloid structure, and the presence of two or only one alkaloid side group defining the catalyst pocket. The conformational rigidity of the linker–ether connections was probed via DFT calculations on the methoxylated models, uncovering especially high barriers to ether rotation out of plane in the arene systems that include the pyridazine ring. These linkers are also found in the catalysts with the highest enantioinduction. The diversity of the SER results suggested that the three apparently analogous test reactions may proceed by significantly different mechanisms. Based on these findings, a stripped-down analogue of  $(\text{DHQD})_2\text{PYDZ}$ , termed “ $(\text{trunc})_2\text{PYDZ}$ ”, was designed, synthesized, and evaluated, showing modest but considerable asymmetric induction in the three test reactions, with the best performance on the 1,1-disubstituted alkeneamide cyclization. This first effort to map out the factors essential to effective stereocontrol and reaction promotion offers guidance for the simplified design and systematic refinement of new, selective organocatalysts.



## INTRODUCTION

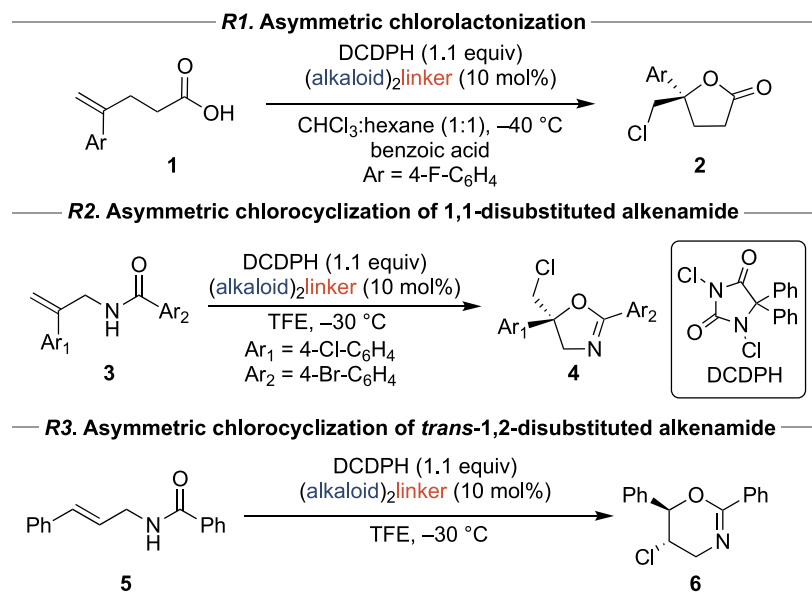
The last decade has seen the emergence of powerful tools for asymmetric halofunctionalization of alkenes. These reactions can rapidly transform relatively simple olefinic substrates into complex scaffolds with multiple stereogenic centers.<sup>1–9</sup> Our first studies uncovered highly stereocontrolled chlorocyclizations of unsaturated carboxylic acids and amides catalyzed by  $(\text{DHQD})_2\text{PHAL}$ , the same organocatalyst used in the venerable Sharpless asymmetric dihydroxylation reaction.<sup>10,11</sup> Mechanistic studies then demonstrated that this catalyst controls the stereochemistry of both halenium ion and nucleophile delivery.<sup>12–15</sup> However, despite the many literature reports on  $(\text{DHQD})_2\text{PHAL}$ -catalyzed halofunctionalization,<sup>3,11,16–20</sup> little is known about the specific structural features of the catalyst that are responsible for asymmetric induction. This report examines the various components of  $(\text{DHQD})_2\text{PHAL}$  to develop structure–enantioselectivity relationships (SERs) for some of the asymmetric halocyclizations we have developed in recent years. As illustrated in Figure 1, the subunits that comprise the catalyst are varied to probe their influence on asymmetric selectivity. This leads to the design of a new potential catalyst that incorporates the minimum required elements.

Using  $(\text{DHQD})_2\text{PHAL}$  as the organocatalyst, our labs have explored stereocontrolled halofunctionalizations with various alkene substrates, chlorenium sources, and nucleophiles. These



**Figure 1.** General structure of cinchona alkaloid dimer catalysts as exemplified with  $(\text{DHQD})_2\text{PHAL}$  structures.

Received: January 12, 2023

Scheme 1. Test Reactions Used for the SER Study of  $(DHQD)_2PHAL$ -Catalyzed Chlorocyclization<sup>a</sup>

<sup>a</sup>Reaction 1 (**R1**) is an example of chlorolactonization. Reaction 2 (**R2**) is an example of chlorocyclization of a 1,1-disubstituted alkeneamide. Reaction 3 (**R3**) is an example of chlorocyclization of a 1,2-disubstituted alkeneamide. DCDPH = 1,3-dichloro-5,5-diphenylhydantoin, TFE = 2,2,2-trifluoroethanol.

Table 1. Effect of Azaaromatic Linker Size on Enantioselectivity<sup>a</sup>

Azaaromatic Linkers				
	PHAL	PYDZ	bzPHAL	NAPY
<b>R1</b>	84	80	85	-59
<b>R2</b>	90	93	86	12
<b>R3</b>	99	98	99	4

<sup>a</sup>Cinchona alkaloid units and azaaromatic linkers. Enantioselectivity of various linkers on reactions **R1–R3** is presented as numbers in the table. DHQD = dihydroquinidine; PHAL = 1,4-linked phthalazine; PYDZ = 3,6-linked pyridazine; bzPHAL = 1,4-linked benzophthalazine; NAPY = 2,7-linked 1,8-naphthyridine.

reactions include chlorocyclizations of alkenoic acids,<sup>10</sup> alkeneamides,<sup>11,21</sup> and alkene carbamates,<sup>19</sup> where the nucleophilic moiety is intramolecular, as well as reactions like chloro-etherification/amidation and dichlorination where nucleophilic attack is intermolecular.<sup>17,22,23</sup> Nicolaou, Hennecke, and other groups have also reported the use of  $(DHQD)_2\text{PHAL}$ -type catalysts for asymmetric halofunctionalizations.<sup>16,18</sup> The sheer numbers of successful applications speak to the robustness and versatility of these cinchona alkaloid catalysts in asymmetric halofunctionalization methodologies.

The structure of  $(DHQD)_2\text{PHAL}$  (Figure 1) consists of two dihydroquinidine (DHQD) alkaloid units linked by phthalazine (PHAL). The alkaloid unit is composed of quinuclidine and methoxyquinoline moieties both connected to a carbinol carbon. In the following sections, any such catalyst with two alkaloid subunits bridged by a linker is denoted as follows:  $(\text{alkaloid})_2\text{linker}$  (Figure 1). Variation of these substructures generates catalyst candidates with a range of functional groups

and conformational possibilities. Structure–enantioselectivity relationships (SER) are mapped using three asymmetric halofunctionalization reactions **R1–R3** (Scheme 1) in which  $(DHQD)_2\text{PHAL}$  is effective. These studies reveal key aspects of catalyst structure, ideally opening the door to optimization of both enantioselectivity and rate, while offering valuable insights into the mechanisms of the probe reactions.

## RESULTS AND DISCUSSION

**SER Studies.** Chlorolactonization<sup>10</sup> and chlorocyclization<sup>11,21</sup> represent some of the earliest reports of catalytic asymmetric chlorofunctionalizations. Here, the product enantioselectivities of these reactions are used in a structure–enantioselectivity relationship (SER) study to explore the effects of catalyst structural variations. The three chosen reactions are **R1**: chlorolactonization of a 1,1-disubstituted alkene-carboxylic acid; **R2**: chlorocyclization of a 1,1-disubstituted alkeneamide; and **R3**: chlorocyclization of a 1,2-disubstituted alkeneamide (Scheme 1). All three occur via

asymmetric delivery of the chlorenium ion to one enantiotopic face of the alkene, which we have suggested is activated by the alkene's proximity to the internal nucleophile (carbonyl oxygen).<sup>12,24</sup> For this SER study, the original conditions for **R1**, **R2**, and **R3** were modified slightly to establish identical initial concentrations of catalysts and reactants across the different reactions. Under these new standard conditions, and with  $(\text{DHQD})_2\text{PHAL}$  as catalyst, reactions **R1**, **R2**, and **R3** yielded asymmetric products with 84, 90, and 99% *ee*, respectively (Table 1).

Cinchona alkaloid dimers, and in particular  $(\text{DHQD})_2\text{PHAL}$ , were among the first organocatalysts to successfully catalyze asymmetric halofunctionalization chemistry. To establish SERs for the halocyclizations **R1**–**R3**, various structural elements of the catalysts were interrogated. Inspired by the classic  $(\text{DHQD})_2\text{PHAL}$ , the catalysts in this work were built on the motif of a central linker (like PHAL) flanked by a pair of chiral moieties (like DHQD), attached via ether linkages. Structural components and aspects investigated were the linker (addressing size and the presence of aromatic  $\text{sp}^2$  nitrogen atoms), the quinuclidine (substituents,  $\text{sp}^3$  nitrogen atoms, chiral centers C8 and C9, see Figure 1), and the quinoline (substituent steric and electronic effects).

SER for **R1**–**R3** showed variable sensitivities to linker rigidity and polarity, aspects of the alkaloid structure, and the presence of two or only one alkaloid side group defining the catalytic site. The conformational rigidity of the linker–ether connections was probed via DFT calculations on methoxylated linker models, uncovering especially high barriers to ether rotation out of plane in the arene systems that include the pyridazine ring. These linkers are also found in the catalysts with the highest enantioinduction. Based on these findings, a stripped-down analogue of  $(\text{DHQD})_2\text{PYDZ}$ , termed “(trunc)<sub>2</sub>PYDZ”, was designed, synthesized, and evaluated, showing modest but substantial asymmetric induction in the three test reactions, with the best performance on the 1,1-disubstituted alkene amide cyclization.

Importantly, this work is the first analysis of its kind as applied to stereocontrolled halofunctionalizations. Though these reactions have catalysts in common with the long-studied (and mechanistically challenging) Sharpless asymmetric alkene dihydroxylation, they differ in essentially all other aspects. Indeed, the diversity of the SER results among **R1**–**R3** suggests that even these three apparently analogous test reactions proceed by significantly different mechanisms. By mapping out the factors essential to effective stereocontrol and reaction promotion, the results offer guidance for the simplified design and systematic refinement of new, selective organocatalysts.

**Size of the Linker.** At the center of the catalyst, the linker holds the two cinchona alkaloid units together in the required geometry. Therefore, we began our study with a structural investigation of the linker size. Two new catalysts,  $(\text{DHQD})_2\text{PYDZ}$  and  $(\text{DHQD})_2\text{bzPHAL}$ , were synthesized, where the linker size was varied while retaining the dihydroquinidine (DHQD) moiety. The two linkers consisted of a pyridazine (PYDZ) and a benzophthalazine (bzPHAL), smaller and larger analogues of the original phthalazine (PHAL) linker. As shown in Table 1, compared to reactions catalyzed by  $(\text{DHQD})_2\text{PHAL}$ , **R1** suffered a small but measurable erosion of the enantioselectivity with the smaller linker, giving 80% *ee* with  $(\text{DHQD})_2\text{PYDZ}$ , whereas  $(\text{DHQD})_2\text{bzPHAL}$  with the larger linker gave 85% *ee*, a slight

improvement. **R2** displayed the reverse trend, showing improvement with the smaller linker and erosion with the larger one. **R3** showed no measurable dependency on linker size.

Having found only modest effects upon elongating or shortening the diazaaromatic linker “floor” of the catalytic binding pocket, we next considered the consequences of widening it by introducing a 1,8-naphthyridine (NAPY) linker. The resulting catalyst,  $(\text{DHQD})_2\text{NAPY}$  (Table 1) retains the two  $\text{sp}^2$  nitrogen atoms embedded in the bicyclic naphthalene framework of the linker, but in positions different from those in PHAL (2,3-diazanaphthalene). The linker holds the two alkaloid units further apart and at a different angle. This modification flipped the enantioselectivity for **R1** from 84% *ee* (with  $(\text{DHQD})_2\text{PHAL}$ ) to a nontrivial –59% *ee*. Reactions **R2** and **R3**, however, completely lost selectivity, giving nearly racemic product. Viewed in the best light, these findings offer a simple way of switching the enantioselectivity of the product without resorting to switching the chirality of the  $(\text{DHQD})_2\text{PHAL}$  catalyst itself. They also point to substantial differences between the stereochemical control elements of **R1** vs **R2** and **R3**. Specifically, they support the idea that  $\pi$ – $\pi$  stacking<sup>25</sup> may play a more significant role in substrate orientation in the catalyst cleft for **R1** than for **R2** and **R3**.

**Role of the Phthalazine Nitrogen Atoms.** To uncover the essential aspects of the linker and the role of the phthalazine nitrogen atoms, we synthesized and tested several (alkaloid)<sub>2</sub>linker systems with nitrogen-free linkers. As summarized in Table 2, when attached to the phthalazine linker, the alkaloid subunits DHQD, QD, and DHQ notably all gave similar (~80%) absolute enantioselectivities in **R1**, enabling fair comparisons across  $(\text{DHQD})_2\text{PHAL}$ ,  $(\text{QD})_2\text{PHAL}$ , and  $(\text{DHQ})_2\text{PHAL}$ , the “pseudoenantiomer” of  $(\text{DHQD})_2\text{PHAL}$ . Replacement of the phthalazine in  $(\text{DHQD})_2\text{PHAL}$  with a simple naphthalene linker formed the deaza analogue,  $(\text{DHQD})_2\text{NAPH}$  (see Table 2 for structures). This catalyst led to low selectivities in **R1**, **R2**, and **R3**. Somewhat surprising, however, was the inversion of selectivity of **R2**. The even simpler 1,4-benzene bridged  $(\text{QD})_2\text{C}_6\text{H}_4$  was essentially catalytically incompetent for stereoinduction, showing only slight positive selectivity in **R2**. Speculating that fluorination might introduce additional hydrogen bonding interactions or mimic the electron-withdrawing effect of the nitrogen atoms, we also explored the tetrafluorinated analogue  $(\text{QD})_2\text{C}_6\text{F}_4$ , again finding low, but now inverted, selectivities for all three reactions (Table 2). Similarly, replacement of the phthalazine linker of  $(\text{DHQ})_2\text{PHAL}$  with anthraquinone (AQN) led to a near-complete loss in selectivity for **R1** and **R2**, from –77 to –12% *ee* and from –95 to –5% *ee*, respectively. Interestingly, for **R3**, enantioselectivity was inverted from –99 to 35% *ee*. Studying asymmetric dichlorination of allylic alcohols, the Nicolaou group noted losses like those above in switching from  $(\text{DHQ})_2\text{PHAL}$  to  $(\text{DHQ})_2\text{AQN}$ .<sup>16</sup> They proposed that the nitrogen atoms in the linker were involved in hydrogen bonding with the allylic alcohol in the transition state, while the quinuclidine moiety of the catalyst delivered the chlorenium source to the more accessible face of the alkene. Analogous interactions could be envisioned between the substrates for reactions **R1**–**R3** and the PHAL linker nitrogen atom in the catalyst; this binding mode would be lost upon replacement of PHAL with AQN. It is worth mentioning that for the Sharpless asymmetric dihydroxylation, the commer-

**Table 2. Enantioselectivity Using Linkers without Aromatic Nitrogen<sup>a</sup>**

Alkaloid Units			
DHQD	QD (R = H) Me <sub>2</sub> QD (R = Me)	DHQ	
Deazaaromatic Linkers			
NAPH	C <sub>6</sub> H <sub>4</sub>	C <sub>6</sub> F <sub>4</sub>	AQN
(DHQD) <sub>2</sub> PHAL	(QD) <sub>2</sub> PHAL	(Me <sub>2</sub> QD) <sub>2</sub> PHAL	(DHQ) <sub>2</sub> PHAL
R1	84	81	85
R2	90	86	81 <sup>b</sup>
R3	99	99	99 <sup>b</sup>
(DHQD) <sub>2</sub> NAPH	(QD) <sub>2</sub> C <sub>6</sub> H <sub>4</sub>	(QD) <sub>2</sub> C <sub>6</sub> F <sub>4</sub>	(DHQ) <sub>2</sub> AQN
R1	7	0	-18
R2	-14	12	-9
R3	15	0	-5
			35

<sup>a</sup>Deazaaromatic linkers. NAPH = 1,4-linked naphthalene; C<sub>6</sub>H<sub>4</sub> = 1,4-linked benzene; C<sub>6</sub>F<sub>4</sub> = 1,4-linked tetrafluorobenzene; AQN = 1,4-linked anthraquinone; DHQD = dihydroquinidine; QD = quinidine; Me<sub>2</sub>QD = dimethylquinidine; DHQ = dihydroquinine; PHAL = 1,4-linked phthalazine. <sup>b</sup>These values were obtained with the closely analogous (Me<sub>2</sub>QD)<sub>2</sub>PYDZ catalyst.

cially available (DHQ)<sub>2</sub>AQN gives superior results with alkyl-substituted olefins with comparable results to (DHQD)<sub>2</sub>PHAL, but is less effective for aryl olefins.<sup>26</sup>

The above findings confirm that the nitrogen atoms in the PHAL or PYDZ linker are important structural components of the catalyst for asymmetric chlorofunctionalizations. Though they may participate in hydrogen bonding, another important function is to rigidify the catalyst. The two ether oxygens that connect the PHAL or PYDZ linker to the alkaloid unit prefer a geometry coplanar to the PHAL ring due presumably to delocalization of the oxygen 2p lone pair electrons into the C—N  $\pi^*$  orbital in the ring. Meanwhile, as in carboxylic esters, the stereoelectronic preference of oxygen's  $sp^2$  (in-plane) lone pair is to lie *anti* to the C—N bond. These effects strongly favor a parallel and coplanar arrangement of the linker—O—C<sub>alkaloid</sub> ether moieties. To explore this issue further, we resorted to computational modeling at the B3LYP-D3/6-31+G\* level of theory. Figure 2 shows calculated potential energy functions for rotation of a single methoxy group in the dimethoxylated analogues (e.g., 1,4-dimethoxyphthalazine) for seven of the linkers that are 1,4-disubstituted with alkaloid groups. Upon rotation out of the plane, the diaza linkers all show a much steeper rise in energy than the carbocyclic linkers, reflecting their stronger preference for the in-plane geometry. The latter trend holds true across analogues of the same ring size (PYDZ vs C<sub>6</sub>H<sub>4</sub> and C<sub>6</sub>F<sub>4</sub>, PHAL vs NAPH, and bzPHAL vs AQN). Similar observations from the literature<sup>27</sup> support the hypothesis that a key role of the linker nitrogen atom is to

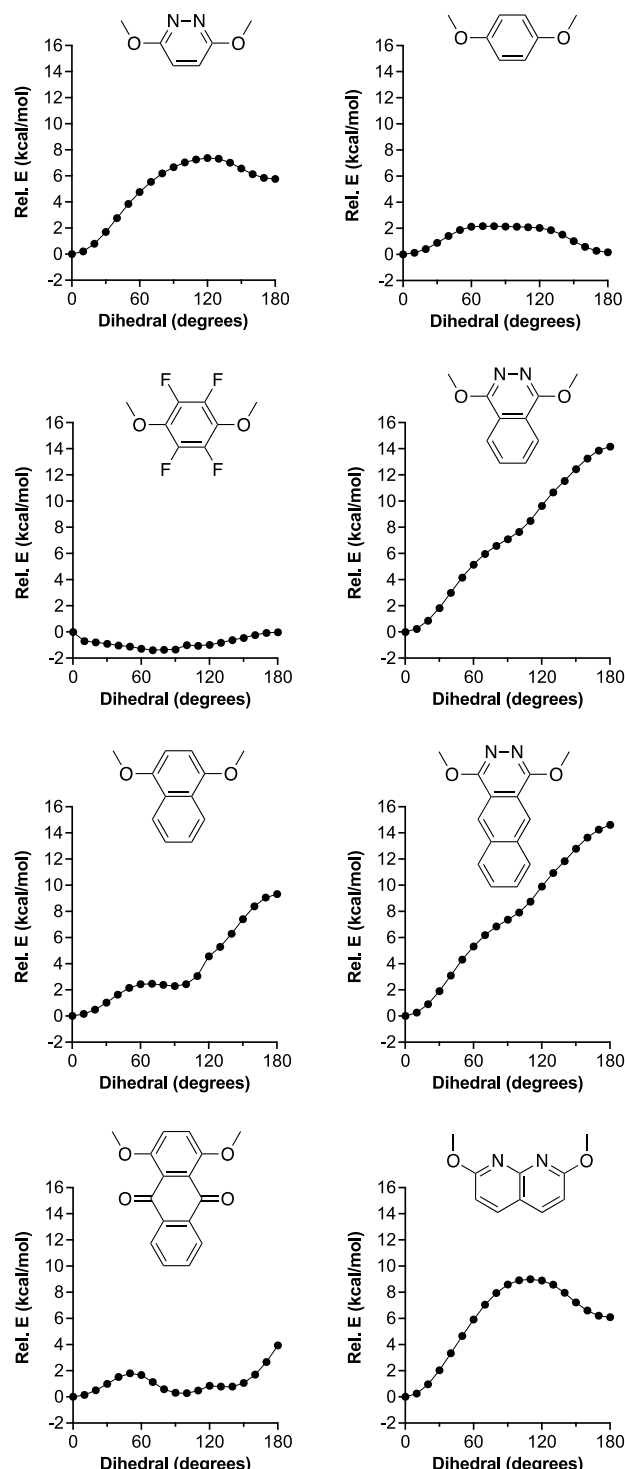


**Figure 2.** B3LYP-D3/6-31+G\* energy profiles for C—O bond rotations of one of the methoxy groups in each of the dimethoxylated linkers shown. Vertical axes are in kcal/mol, and horizontal axes represent N=C—O—C(H<sub>3</sub>) or analogous dihedral angles such that 0° corresponds to the methoxy carbon lying coplanar to the ring as depicted. Except for the C—O torsion angle of the methoxy group being constrained, structures were fully relaxed at each step. Particularly surprising was the 1,4-dimethoxy-9,10-anthroquinone linker (bottom left); in a more comprehensive search, between competing resonance, dipole–dipole, and steric interactions, this compound shows no less than nine symmetry-distinct conformational minima, all within  $\leq 2.5$  kcal/mol.

Table 3. Effect of Quinuclidine Nitrogen Atoms on Enantioselectivity<sup>a</sup>

	Alkaloid Units		
	DHQD-EtI	DHQD-BnBr	(QD)(Cl)PYDZ
	(DHQD)(DHQD-EtI)PHAL	(DHQD)(DHQD-BnBr)PHAL	(QD)(Cl)PYDZ
<i>R1</i>	57	51	1
<i>R2</i>	80	87	51
<i>R3</i>	98	83	24

<sup>a</sup>DHQD = dihydroquinidine; QD = quinidine; PYDZ = 3,6-linked pyridazine; PHAL = 1,4-linked phthalazine.

rigidify the structures, holding the two cinchona alkaloid fragments via ether linkages that lie in the plane of the linker arene. This structural element defines the chiral pocket. Linkers without the nitrogen atoms lack this rigidity, and thus the structural definition, needed for catalytic stereodifferentiation. Though the low ( $\leq 3$  kcal/mol) variations in energy across the methoxy rotations in 1,4-dimethoxybenzene ( $C_6H_4$  linker) and 1,2,4,5-tetrafluoro-3,6-dimethoxybenzene ( $C_6F_4$  linker) were unsurprising, the similarly low ( $\leq 4$  kcal/mol) variations in the 1,4-dimethoxyanthracene-9,10-dione (AQN linker) case were striking. A complete conformational analysis (see the SI) of this compound found at least nine symmetry unique (i.e., not counting enantiomeric pairs) conformational minima, all within  $\leq 2.5$  kcal/mol of the lowest energy! The reader is referred to the SI for a proposed stereochemical explanation of the latter observation.

**Role of the Quinuclidine Nitrogen Atom.** The quinuclidine moiety itself includes several chiral centers along with a basic,  $sp^3$  nitrogen atom, which may play an important role in substrate orientation and alkene activation. Previous reports on Sharpless asymmetric dihydroxylation have shown that this quinuclidine moiety coordinates to the osmium metal center.<sup>28</sup>

For the present chlorocyclizations, it has been suggested that the quinuclidine nitrogen atom may coordinate to the electrophilic chlorine source or even abstract the chlorenium ion itself before delivering it to the alkene. Nonetheless, based on our previously reported NMR and stereochemical results<sup>14</sup> the alkene-carboxylic acid substrate in *R1* binds more tightly to the strongly basic quinuclidine site than DCDMH (1,3-dichloro-5,5-dimethylhydantoin), the chlorenium ion donor. Thus, the quinuclidine nitrogen atom on the catalyst likely plays a key substrate recognition role via hydrogen bonding.

To probe the importance of the quinuclidine nitrogen atoms in the catalytic function of  $(DHQD)_2PHAL$ , two derivatives in which one of the two quinuclidine sites was alkylated were prepared. These mono *N*-alkylammonium salts, (DHQD)-(DHQD-EtI)PHAL and (DHQD)(DHQD-BnBr)PHAL, displayed significant reductions in enantioselectivity for *R1*, giving 57% ee for the *N*-ethylated and 51% ee for the *N*-benzylated catalysts (Table 3). Nonetheless, the significant residual enantioselectivity suggested that the remaining unmodified dihydroquinidine moiety was still able to achieve some stereoselective catalytic function. Meanwhile, *R2* and *R3* showed minimal loss of enantioselectivity with the quaternized catalysts. These findings suggest that only one quinuclidine nitrogen atom is involved in the catalytic processes of *R2* and

*R3*, whereas *R1* is more sensitive. More broadly, they hint that the catalytic pathways for *R2* and *R3* may differ from what has been proposed for *R1*.<sup>14</sup> Potential roles for the alkylated quinuclidine moieties could not be probed, as a synthesis of catalysts where both quinuclidine nitrogen atoms were alkylated led to unstable products that could not be purified to homogeneity.

**Is the Second Alkaloid Unit Necessary?** The quinuclidine quaternization results suggested that the second quinuclidine nitrogen atom might not be needed for catalytic efficacy. To explore this issue, the “half” catalyst (QD)(Cl)-PYDZ was synthesized and tested. This catalyst lacked one of the alkaloid (QD) units, which was replaced simply with a chlorine atom. As seen in Table 3, with (QD)(Cl)PYDZ as catalyst, *R1* lost all selectivity, while *R2* and *R3* retained modest and low stereoselectivities, respectively. Evidently, the second alkaloid unit, while not essential for reaction, does play a role in controlling the asymmetric induction, perhaps by placing steric boundaries on the chiral pocket of the catalyst. It should be noted, however, that Hennecke and co-workers have had success with similar catalysts for the dichlorination of styrenyl systems.<sup>29</sup>

**Role of the Quinuclidine Substituent.** The quinuclidine moiety in the dihydroquinidine alkaloid fragment (DHQD) includes an unfunctionalized ethyl substituent at C3 (Figure 1). To test the effect of this ethyl fragment on stereoselectivity, the entire (DHQD) fragment was replaced with commercially available quinidine (QD). Replacing DHQD with QD resulted in the catalysts (QD)<sub>2</sub>PHAL or (QD)<sub>2</sub>PYDZ. For *R1*, this modification led to 3 and 4% drops in enantioselectivity for the PHAL and PYDZ linkers, respectively. Similar results were seen for *R2* and *R3* with negligible effects on stereoinduction (Tables 2 and 4). These small changes in selectivity are not surprising given that ethyl and vinyl groups are not drastically different in steric size. However, the low sensitivity of product enantioselectivity toward linker and alkaloid substitution does have some practical implications: (1) various quinidine alkaloids and linkers are commercially available, offering opportunities to create new potential catalysts, and (2) compared to (DHQD)<sub>2</sub>PHAL, alkaloid dimers like (QD)<sub>2</sub>PYDZ are structurally somewhat simpler, easier to prepare, and more readily functionalized on both the quinuclidine substituent and the linker ring to generate novel catalytic systems. Such elaboration is demonstrated in the (Me<sub>2</sub>QD)<sub>2</sub>PYDZ catalyst, a modified derivative of the (QD)<sub>2</sub>PYDZ system, which was easily synthesized using Grubbs metathesis.<sup>30</sup> Corey et al. had also exploited this ease

**Table 4. Effect of Substituent Size at C3 Position of Quinuclidine<sup>a</sup>**

Alkaloid Units			
	DHQD	QD	Me <sub>2</sub> QD
(QD) <sub>2</sub> PHAL	81	76	80
(QD) <sub>2</sub> PYDZ		88	86
(QD) <sub>2</sub> bzPHAL			71
(Me <sub>2</sub> QD) <sub>2</sub> PYDZ			99
<i>R1</i>	81	76	84
<i>R2</i>	86	88	86
<i>R3</i>	99	99	99

<sup>a</sup>DHQD = dihydroquinidine; QD = quinidine; Me<sub>2</sub>QD = dimethylquinidine; PHAL = 1,4-linked phthalazine; PYDZ = 3,6-linked pyridazine; bzPHAL = 1,4-linked benzophthalazine.

of functionalization, synthesizing a cyclic derivative of the (QD)<sub>2</sub>PYDZ system<sup>31</sup> with a long-chain bridge joining the quinuclidine substituent sites. Despite the smaller PYDZ linker, for *R1*, the (Me<sub>2</sub>QD)<sub>2</sub>PYDZ catalyst showed the same selectivity as the parent (DHQD)<sub>2</sub>PHAL. Overall, (Me<sub>2</sub>QD)<sub>2</sub>PYDZ was found to have comparable selectivity to (QD)<sub>2</sub>PYDZ, further confirming that the C3 substituent (e.g., the ethyl group in (DHQD)<sub>2</sub>PHAL) has only a small impact on stereoselectivity (Table 4). These findings are also consistent with the relatively small differences in absolute selectivity between (DHQD)<sub>2</sub>PHAL and (DHQ)<sub>2</sub>PHAL, “pseudoenantiomer” catalysts whose only deviation from a true enantiomeric relationship is in the configuration of the ethyl attachments on the quinuclidine moieties.

#### Role of the C8/C9 Relative Stereochemistry.

(DHQD)<sub>2</sub>PHAL and (DHQ)<sub>2</sub>PHAL exhibit nearly complete reversal in their selectivity toward *R1*, *R2*, and *R3* (Table 2). As noted above, these two catalysts have opposite configurations at the C8 and C9 alkaloid stereocenters but the same configurations at the ethyl connection to the quinuclidine. Thus, the C8 and C9 stereocenters appear to be the most important for shaping the chiral pocket leading to enantioselectivity. To explore this hypothesis, the (C9-*epi*-DHQD)<sub>2</sub>PYDZ was synthesized and tested on all three reactions (Table 5). Compared to the respectable enantioselectivity obtained with (DHQD)<sub>2</sub>PYDZ (Table 5; 80, 93, and 98% ee for *R1*–*R3*, respectively), *R1* and *R3* lost nearly all selectivity, but *R2* retained more than half (57 vs 93%) when catalyzed with the (C9-*epi*-DHQD)<sub>2</sub>PYDZ. This trend appears similar to the results seen with (QD)(Cl)PYDZ, where removal of one of the alkaloid units led to drastic selectivity losses for *R1* and *R3*, but less for *R2* (see Table 3). Since this catalyst was expected to have a significantly redefined chiral pocket, these results may suggest that the selectivity in *R2* is dominated by more localized substrate–catalyst interactions than in *R1* and *R3*, and further supports the hypothesis that the second alkaloid unit (DHQD or QD) simply shapes the chiral cavity. Modification of the C9 stereocenters presumably reorients the quinuclidines, moving the locus of the reaction out from binding in the chiral pocket.

**Steric Effects of Quinoline Ring Substituents.** The mechanistic picture proposed for the Sharpless asymmetric dihydroxylation of styrenyl substrates invokes a π–π stacking interaction between the quinoline moiety of (DHQD)<sub>2</sub>PHAL

**Table 5. Effect of the C8/C9 Relative Stereochemistry on Enantioselectivity<sup>a</sup>**

Alkaloid Units		
	DHQD	DHQ
(DHQD) <sub>2</sub> PYDZ	80	–77
(DHQ) <sub>2</sub> PHAL	93	–95
(C9- <i>epi</i> -DHQD) <sub>2</sub> PYDZ	98	–99
<i>R1</i>	80	11
<i>R2</i>	93	57
<i>R3</i>	99	17

<sup>a</sup>DHQD = dihydroquinidine; DHQ = dihydroquinine; PYDZ = 3,6-linked pyridazine; PHAL = 1,4-linked phthalazine; *epi*-DHQD = C9-*epi*-epimer of dihydroquinidine.

and an aromatic ring of the substrates.<sup>25</sup> These π–π- or CH–π-type weak interactions could be present in the asymmetric chlorofunctionalization processes as well. In fact, most of the reported alkene substrates have a neighboring aromatic moiety,<sup>32</sup> suggesting that the catalyst could benefit from such interactions. To test this idea, we synthesized two new catalysts (CN)<sub>2</sub>PYDZ and (iPr-DHQD)<sub>2</sub>PYDZ, where the methoxy groups of the original DHQD moieties had been replaced by H and by isopropoxy groups, respectively, thus modifying the steric and electronic environment of the catalyst binding pocket. Surprisingly, both catalysts displayed lower selectivity than (DHQD)<sub>2</sub>PYDZ for *R1* (Table 6). This can be

**Table 6. Effect of Quinoline Size and Electronics on Enantioselectivity; Alkaloids with Modified Quinoline<sup>a</sup>**

Alkaloid Units		
	DHQD	iPr-DHQD
(DHQD) <sub>2</sub> PYDZ	80	58
(iPr-DHQD) <sub>2</sub> PYDZ	93	97
(CN) <sub>2</sub> PYDZ	98	99
<i>R1</i>	80	65
<i>R2</i>	93	91
<i>R3</i>	98	98

<sup>a</sup>DHQD = dihydroquinidine; CN = chinconine; PYDZ = 3,6-linked pyridazine.

rationalized in the following way: due to its increased bulk, (iPr-DHQD)<sub>2</sub>PYDZ disrupts any π–π or CH–π interactions needed for optimum selectivity. (CN)<sub>2</sub>PYDZ does not suffer from such steric hindrance, but removal of the electron-rich alkoxy group may change the electronics of the quinoline ring enough for it to weaken π–π interactions with the substrate due to its less polar and polarizable π-system. Neither *R2* nor *R3* showed any significant change in selectivity in either case, suggesting that such catalyst–substrate interactions are absent or at least unaffected by the changes in the catalyst. These data are in accordance with our earlier reports where the substrates with cyclohexyl instead of aryl groups gave poor enantiose-

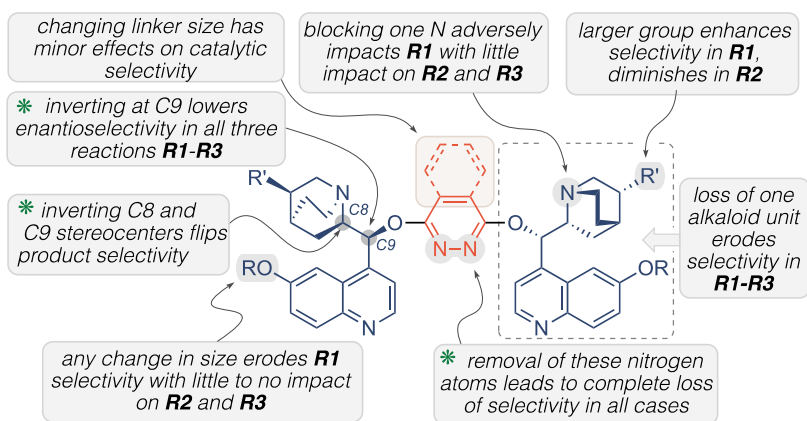


Figure 3. Summary of SER studies on cinchona alkaloid catalyst (\* denotes the critical features that affect stereoinduction).

Table 7. Effect of Ester-Based Linkers on Enantioselectivity<sup>a</sup>

Ester Linkers						
<b>PHTHAL</b>	<b>isoPHTHAL</b>	<b>TERE</b>	<b>SUCC</b>	<b>GLUT</b>	<b>ADI</b>	
(QD) <sub>2</sub> PHTHAL	(QD) <sub>2</sub> isoPHTHAL	(QD) <sub>2</sub> TERE	(QD) <sub>2</sub> SUCC	(QD) <sub>2</sub> GLUT	(QD) <sub>2</sub> ADI	
<b>R1</b>	3	38	2	1	2	1
<b>R2</b>	48	15	47	75	46	57
<b>R3</b>	44	48	51	60	48	43

<sup>a</sup>PHTHAL = phthaloyl linked; isoPHTHAL = *i*-phthaloyl linked; TERE = terephthaloyl linked; SUCC = succinyl linked; GLUT = glutaroyl linked; ADI = adipoyl linked; QD = quinidine.

lectivity for **R1** but high enantioselectivity for **R3**, implying different roles for  $\pi-\pi$  stacking in **R1** versus **R3**.<sup>10,11</sup>

**Summary of Structural Variations.** Variations of the substituent on the quinuclidine or the configuration of its attachment make only modest changes to the catalyst's enantioselectivities. **R2** and **R3** (but not **R1**) are also relatively insensitive to steric or electronic changes on the quinoline ring. Likewise, varying the length of the PHAL analogue linkers (PYDZ and BzPHAL) retains the selectivities seen with PHAL. These findings broaden the catalyst design palette to include various alternative, commercially available, or laboratory-modified catalysts for these halofunctionalization reactions without sacrificing catalyst efficacy. On the other hand, the presence of aromatic nitrogen atoms in a linker of appropriate width is essential for effective stereoselectivity. The other influential elements are the relative configurations of the C8 and C9 stereocenters adjacent to the linker. Catalysts diastereomeric at C8/C9 show greatly eroded selectivity. Notably, for **R1**, modification of the catalyst geometry by use of the NAPY linker reverses the enantioselectivity despite the alkaloid subunits' chirality being unchanged. Given the  $C_2$ -symmetric structure of the (DHQD)<sub>2</sub>PHAL parent catalyst, we envision that one of the two quinuclidine moieties might create a wall that defines the substrate binding pocket, without being involved in direct coordination or activation processes during the catalysis. Therefore, both alkaloid units are necessary to retain proper catalyst functioning, as removing one unit can render the catalyst unselective. Considering the test reactions, **R1** appears to be the most sensitive to catalyst structural modifications, whereas **R2** and **R3** are more robust, likely

occurring via more localized interactions with the catalyst structure (see Figure 3 for a pictorial summary).

**Application to Catalyst Design.** To build on the results from the SER studies, we pursued several structural modifications on (QD)<sub>2</sub>PHAL in search of a simpler, functional catalyst structure. We began by replacing the PHAL linker unit. Having noted the structural rigidification due to electron delocalization to the nitrogen atoms of the phthalazine linker (PHAL), we explored its oxygen analogue, the phthalate (benzene *ortho*-dicarboxylate) diester (QD)<sub>2</sub>PHTHAL where the linking oxygen atoms are no longer attached directly to the ring (see Table 7 for structures). The two ester carbonyl groups would therefore likely lie out of the arene plane due to steric and dipole–dipole interactions; nonetheless, their structural relationship should be fairly rigid. Nearly all selectivity was lost for **R1**, presumably due to the loss of structural definition, as was found with the NAPH,  $C_6H_4$ ,  $C_6F_4$ , and AQN linkers. Reactions **R2** and **R3** did retain moderate selectivity, albeit far less than with the best catalysts. Here again, the linker's poor conformational definition was likely enough to disrupt the chiral pocket created by the two alkaloid units, affecting **R1** more severely than **R2** and **R3**. Similar trends in reaction performance were found with the phthalate isomer diester linkers isoPHTHAL and TERE, and with aliphatic backbones in the succinate (SUCC), glutarate (GLUT), and adipate diesters (ADI), with none surpassing the original catalyst efficacy.

**Minimalist Approach to Catalyst Design.** Highlighted in Figure 3 are the components of (DHQD)<sub>2</sub>PHAL with variable influence on the catalytic efficiency for the transformations investigated. Extracting the most influential

components i.e., the linker, the rigidity of the 1,4-substitutions afforded by the diaza aryl group, and the relative configurations at C8 and C9, a trimmed-down version of  $(\text{DHQD})_2\text{PYDZ}$  was explored (see  $(\text{trunc})_2\text{PYDZ}$  structure in Figure 4). This

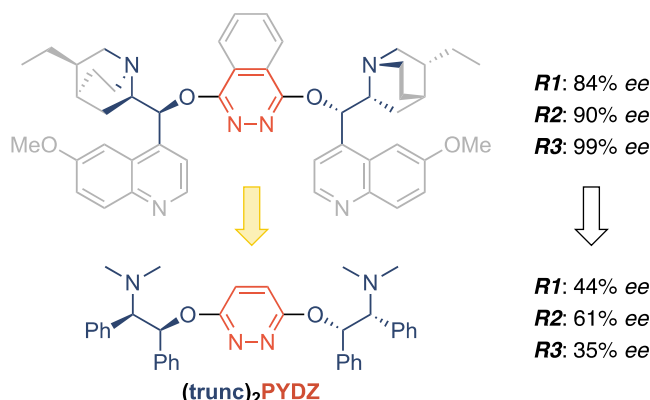


**Figure 4.** Truncated catalyst retains the most critical elements identified in the SER study of  $(\text{DHQD})_2\text{PHAL}$ , leading to appreciable enantio-induction for the three reactions **R1–R3** without structural or reaction optimization efforts. The  $(\text{trunc})_2\text{PYDZ}$  catalyst represents a minimalist approach to catalyst design.

structure contains the most basic elements deemed necessary for imparting stereoselectivity, representing a minimalist approach to the design of a new catalyst framework. The complex quinoline and quinuclidine moieties were omitted, leaving only tertiary amine centers and aromatic rings. Given its radically altered structure and great reduction in bulk, we were pleased that  $(\text{trunc})_2\text{PYDZ}$  led to surprisingly significant *eess* (44, 61, and 35% *ee* for **R1**, **R2**, and **R3**, respectively) for a catalyst lacking any structural optimization. Beyond its value in reconfirming the role of the critical elements that the SER study has revealed, this proof-of-principle result demonstrates the value of SER in guiding the design of simplified catalyst motifs. As a bonus, mechanistic interpretation of these results indicates that for **R1**, the definition of the catalytic pocket plays a major role so that the lack of efficient  $\pi$ – $\pi$  stacking in  $(\text{trunc})_2\text{PYDZ}$  gives eroded enantioselectivity. On the other hand, **R2** is more dependent on local interactions with the stereogenic catalyst functionalities and less on the overall structure and ability to participate in  $\pi$ – $\pi$  stacking interactions. For **R3**, the catalytic pocket is needed for efficient selectivity, and thus the absence of the bulky quinuclidine units results in poor enantioselectivity. This approach to catalyst design could enable rapid exploratory generation of libraries of truncated catalysts via routine chemical transformations, in contrast to the synthetic challenges of modifying a catalyst with the complexity of  $(\text{DHQD})_2\text{PHAL}$ .

## CONCLUSIONS

By exploring the effects of catalyst structural variations on the enantioselectivities of the three halocyclization reactions **R1–R3**, we have identified factors essential for effective asymmetric induction. One key issue is the structural definition conferred by the strong rotational preferences of the azaaromatic linkers; in fact, slight but measurable improvements were seen over the performance of  $(\text{DHQD})_2\text{PHAL}$  itself for reactions **R1** with  $(\text{DHQD})_2\text{bzPHAL}$  and **R2** with  $(\text{DHQD})_2\text{PYDZ}$ . The relative configurations of C8 and C9 are also critical; epimerizing C9 severely eroded selectivity, especially for **R1** and **R3**. Figure 3

summarizes the contributions of different domains of the catalysts on the stereochemical outcome of the three reactions investigated.

The three reactions show widely varying sensitivity to structural changes in the catalysts suggesting nontrivial differences in the details of their catalyzed reaction mechanisms. Reaction **R1** in particular shows a need for activation by catalysts with the two alkaloid moieties in rigid, structurally defined relationships, consistent with our recently reported analysis of its  $(\text{DHQD})_2\text{PHAL}$ -catalyzed reaction mechanism.<sup>14</sup> On the other hand, even with only one alkaloid moiety available as in  $(\text{QD})(\text{Cl})\text{PYDZ}$  and effectively catalyst dimers constructed with alkyl diester linkers SUCC, GLUT, and ADI, **R2** shows enantioselectivities that are substantial, albeit not high enough to be of practical synthetic value. Extension of these ideas to the synthesis of new candidate catalyst forms showed that even simplified systems are capable of nontrivial asymmetric induction. Although none of the more severely altered catalysts or the new designs tested yielded significantly better enantioselectivities than the parent  $(\text{DHQD})_2\text{PHAL}$ , the results described here have established the key variables and set the stage for more detailed mechanistic and simulation studies to guide the design of new, potent halofunctionalization reactions.

## ASSOCIATED CONTENT

### Data Availability Statement

The data underlying this study are available in the published article and its Supporting Information.

### Supporting Information

The Supporting Information is available free of charge at <https://pubs.acs.org/doi/10.1021/acs.joc.3c00084>.

Catalyst synthesis and characterization data, and procedures for reactions **R1–R3** and product analysis (PDF)

## AUTHOR INFORMATION

### Corresponding Authors

James E. Jackson – Department of Chemistry, Michigan State University, East Lansing, Michigan 48824, United States; [orcid.org/0000-0002-4506-7415](https://orcid.org/0000-0002-4506-7415); Email: [jackson@chemistry.msu.edu](mailto:jackson@chemistry.msu.edu)

Babak Borhan – Department of Chemistry, Michigan State University, East Lansing, Michigan 48824, United States; [orcid.org/0000-0002-3193-0732](https://orcid.org/0000-0002-3193-0732); Email: [babak@chemistry.msu.edu](mailto:babak@chemistry.msu.edu)

### Authors

Sarah E. Luderer – Department of Chemistry, Michigan State University, East Lansing, Michigan 48824, United States

Behrad Masoudi – Department of Chemistry, Michigan State University, East Lansing, Michigan 48824, United States

Aritra Sarkar – Department of Chemistry, Michigan State University, East Lansing, Michigan 48824, United States

Calvin Grant – Department of Chemistry, Michigan State University, East Lansing, Michigan 48824, United States

Arvind Jaganathan – Department of Chemistry, Michigan State University, East Lansing, Michigan 48824, United States

Complete contact information is available at:

<https://pubs.acs.org/10.1021/acs.joc.3c00084>

## Notes

The authors declare no competing financial interest.

## ACKNOWLEDGMENTS

Generous support was provided in part by the NIH (GM110525) and the NSF (CHE-1362812).

## REFERENCES

- (1) Landry, M. L.; Burns, N. Z. Catalytic Enantioselective Dihalogenation in Total Synthesis. *Acc. Chem. Res.* **2018**, *51*, 1260.
- (2) Murai, K.; Fujioka, H. Recent progress in organocatalytic asymmetric halocyclization. *Heterocycles* **2013**, *87*, 763.
- (3) Cheng, Y. A.; Yu, W. Z.; Yeung, Y.-Y. Recent advances in asymmetric intra- and intermolecular halofunctionalizations of alkenes. *Org. Biomol. Chem.* **2014**, *12*, 2333.
- (4) Cai, Y.; Liu, X.; Zhou, P.; Feng, X. Asymmetric Catalytic Halofunctionalization of  $\alpha,\beta$ -Unsaturated Carbonyl Compounds. *J. Org. Chem.* **2019**, *84*, 1.
- (5) Hennecke, U. New catalytic approaches towards the enantioselective halogenation of alkenes. *Chem. Asian J.* **2012**, *7*, 456.
- (6) Denmark, S. E.; Kuester, W. E.; Burk, M. T. Catalytic, asymmetric halofunctionalization of alkenes—a critical perspective. *Angew. Chem., Int. Ed.* **2012**, *51*, 10938.
- (7) Castellanos, A.; Fletcher, S. P. Current methods for asymmetric halogenation of olefins. *Chem.—Eur. J.* **2011**, *17*, 5766.
- (8) Chen, G.; Ma, S. Enantioselective halocyclization reactions for the synthesis of chiral cyclic compounds. *Angew. Chem., Int. Ed.* **2010**, *49*, 8306.
- (9) Ashtekar, K. D.; Jaganathan, A.; Borhan, B.; Whitehead, D. C. Enantioselective Halofunctionalization of Alkenes. *Organic Reactions* **2021**, *105*, 1–266.
- (10) Whitehead, D. C.; Yousefi, R.; Jaganathan, A.; Borhan, B. An Organocatalytic Asymmetric Chlorolactonization. *J. Am. Chem. Soc.* **2010**, *132*, 3298.
- (11) Jaganathan, A.; Garzan, A.; Whitehead, D. C.; Staples, R. J.; Borhan, B. A Catalytic Asymmetric Chlorocyclization of Unsaturated Amides. *Angew. Chem., Int. Ed.* **2011**, *50*, 2593.
- (12) Salehi Marzijarani, N.; Yousefi, R.; Jaganathan, A.; Ashtekar, K. D.; Jackson, J. E.; Borhan, B. Absolute and relative facial selectivities in organocatalytic asymmetric chlorocyclization reactions. *Chem. Sci.* **2018**, *9*, 2898.
- (13) Yousefi, R.; Ashtekar, K. D.; Whitehead, D. C.; Jackson, J. E.; Borhan, B. Dissecting the stereocontrol elements of a catalytic asymmetric chlorolactonization: syn addition obviates bridging chloronium. *J. Am. Chem. Soc.* **2013**, *135*, 14524.
- (14) Yousefi, R.; Sarkar, A.; Ashtekar, K. D.; Whitehead, D. C.; Kakeshpour, T.; Holmes, D.; Reed, P.; Jackson, J. E.; Borhan, B. Mechanistic Insights into the Origin of Stereoselectivity in an Asymmetric Chlorolactonization Catalyzed by (DHQD)(2)PHAL. *J. Am. Chem. Soc.* **2020**, *142*, 7179.
- (15) Yousefi, R.; Whitehead, D. C.; Mueller, J. M.; Staples, R. J.; Borhan, B. On the Chlorenium Source in the Asymmetric Chlorolactonization Reaction. *Org. Lett.* **2011**, *13*, 608.
- (16) Nicolaou, K. C.; Simmons, N. L.; Ying, Y.; Heretsch, P. M.; Chen, J. S. Enantioselective Dichlorination of Allylic Alcohols. *J. Am. Chem. Soc.* **2011**, *133*, 8134.
- (17) Soltanzadeh, B.; Jaganathan, A.; Yi, Y.; Yi, H.; Staples, R. J.; Borhan, B. Highly Regio- and Enantioselective Vicinal Dihalogenation of Allyl Amides. *J. Am. Chem. Soc.* **2017**, *139*, 2132.
- (18) Wilking, M.; Daniliuc, C. G.; Hennecke, U. Asymmetric, organocatalytic bromolactonization of allenic acids. *Synlett* **2014**, *25*, 1701.
- (19) Garzan, A.; Jaganathan, A.; Salehi Marzijarani, N.; Yousefi, R.; Whitehead, D. C.; Jackson, J. E.; Borhan, B. Solvent-dependent enantiodivergence in the chlorocyclization of unsaturated carbamates. *Chem.—Eur. J.* **2013**, *19*, 9015.
- (20) Yin, Q.; You, S.-L. Enantioselective Chlorocyclization of Indole-Derived Benzamides for the Synthesis of Spiro-indolines. *Org. Lett.* **2013**, *15*, 4266.
- (21) Jaganathan, A.; Staples, R. J.; Borhan, B. Kinetic resolution of unsaturated amides in a chlorocyclization reaction: concomitant enantiomer differentiation and face selective alkene chlorination by a single catalyst. *J. Am. Chem. Soc.* **2013**, *135*, 14806.
- (22) Soltanzadeh, B.; Jaganathan, A.; Staples, R. J.; Borhan, B. Highly Stereoselective Intermolecular Haloetherification and Haloesterification of Allyl Amides. *Angew. Chem., Int. Ed.* **2015**, *54*, 9517.
- (23) Steigerwald, D. C.; Soltanzadeh, B.; Sarkar, A.; Morgenstern, C. C.; Staples, R. J.; Borhan, B. Ritter-Enabled Catalytic Asymmetric Chloroamidation of Olefins. *Chem. Sci.* **2021**, *12*, 1834.
- (24) Ashtekar, K. D.; Vetticatt, M.; Yousefi, R.; Jackson, J. E.; Borhan, B. Nucleophile-Assisted Alkene Activation: Olefins Alone Are Often Incompetent. *J. Am. Chem. Soc.* **2016**, *138*, 8114.
- (25) Corey, E. J.; Guzmanperez, A.; Noe, M. C. The Application of a Mechanistic Model Leads to the Extension of the Sharpless Asymmetric Dihydroxylation to Allylic 4-Methoxybenzoates and Conformationally Related Amine and Homoallylic Alcohol Derivatives. *J. Am. Chem. Soc.* **1995**, *117*, 10805.
- (26) Becker, H.; Sharpless, K. B. A new ligand class for the asymmetric dihydroxylation of olefins. *Angew. Chem., Int. Ed.* **1996**, *35*, 448.
- (27) Becker, H.; Ho, P. T.; Kolb, H. C.; Loren, S.; Norrby, P. O.; Sharpless, K. B. Comparing 2 Models for the Selectivity in the Asymmetric Dihydroxylation Reaction (Ad). *Tetrahedron Lett.* **1994**, *35*, 7315.
- (28) Nelson, D. W.; Gypser, A.; Ho, P. T.; Kolb, H. C.; Kondo, T.; Kwong, H. L.; McGrath, D. V.; Rubin, A. E.; Norrby, P. O.; Gable, K. P.; Sharpless, K. B. Toward an understanding of the high enantioselectivity in the osmium-catalyzed asymmetric dihydroxylation. 4. Electronic effects in amine-accelerated osmylations. *J. Am. Chem. Soc.* **1997**, *119*, 1840.
- (29) Wedek, V.; Van Lommel, R.; Daniliuc, C. G.; De Proft, F.; Hennecke, U. Organocatalytic, Enantioselective Dichlorination of Unfunctionalized Alkenes. *Angew. Chem., Int. Ed.* **2019**, *58*, 9239.
- (30) Qi, J.; Beeler, A. B.; Zhang, Q.; Porco, J. J. A. Catalytic Enantioselective Alkylation Dearomatization—Annulation: Total Synthesis and Absolute Configuration Assignment of Hyperibone K. *J. Am. Chem. Soc.* **2010**, *132*, 13642.
- (31) Corey, E. J.; Noe, M. C. Rigid and highly enantioselective catalyst for the dihydroxylation of olefins using osmium tetroxide clarifies the origin of enantiospecificity. *J. Am. Chem. Soc.* **1993**, *115*, 12579.
- (32) Noe, M. C.; Letavic, M. A.; Snow, S. L. *Organic Reactions* **2005**, *109*.